EUROPEAN ORGANIZATION FOR NUCLEAR RESEARCH

CERN-EP-2002-022
11 March 2002

Measurement of the Mass of the W Boson in e^+e^- Collisions using the Fully Leptonic Channel

The OPAL Collaboration

Abstract

A novel method of determining the mass of the W boson in the $W^+W^- \to \ell\nu\ell'\nu'$ channel is presented and applied to 667 pb^{-1} of data recorded at center-of-mass energies in the range 183–207 GeV with the Opal detector at LEP. The measured energies of charged leptons and the results of a new procedure based on an approximate kinematic reconstruction of the events are combined to give:

$$M_W = 80.41 \pm 0.41 \pm 0.13 \text{ GeV},$$

where the first error is statistical and the second is systematic. The systematic error is dominated by the uncertainty on the lepton energy, which is calibrated using data, and the parameterization of the variables used in the fitting, which is obtained using Monte Carlo events. Both of these are limited by statistics.

(To be submitted to Euro. Phys. J.)

The OPAL Collaboration

G. Abbiendi[2], C. Ainsley[5], P.F. Åkesson[3], G. Alexander[22], J. Allison[16], G. Anagnostou[1], K.J. Anderson[9], S. Asai[23], D. Axen[27], G. Azuelos[18,a], I. Bailey[26], E. Barberio[8], R.J. Barlow[16], R.J. Batley[5], P. Bechtle[25], T. Behnke[25], K.W. Bell[20], P.J. Bell[1], G. Bella[22], A. Bellerive[6], G. Benelli[4], S. Bethke[32], O. Biebel[32], I.J. Bloodworth[1], O. Boeriu[10], P. Bock[11], D. Bonacorsi[2], M. Boutemeur[31], S. Braibant[8], L. Brigliadori[2], R.M. Brown[20], K. Buesser[25], H.J. Burckhart[8], J. Cammin[3], S. Campana[4], R.K. Carnegie[6], B. Caron[28], A.A. Carter[13], J.R. Carter[5], C.Y. Chang[17], D.G. Charlton[1,b], I. Cohen[22], A. Csilling[8,g], M. Cuffiani[2], S. Dado[21], G.M. Dallavalle[2], S. Dallison[16], A. De Roeck[8], E.A. De Wolf[8], K. Desch[25], M. Donkers[6], J. Dubbert[31], E. Duchovni[24], G. Duckeck[31], I.P. Duerdoth[16], E. Etzion[22], F. Fabbri[2], L. Feld[10], P. Ferrari[12], F. Fiedler[8], I. Fleck[10], M. Ford[5], A. Frey[8], A. Fürtjes[8], P. Gagnon[12], J.W. Gary[4], G. Gaycken[25], C. Geich-Gimbel[3], G. Giacomelli[2], P. Giacomelli[2], M. Giunta[4], J. Goldberg[21], E. Gross[24], J. Grunhaus[22], M. Gruwé[8], P.O. Günther[3], A. Gupta[9], C. Hajdu[29], M. Hamann[25], G.G. Hanson[12], K. Harder[25], A. Harel[21], M. Harin-Dirac[4], M. Hauschild[8], J. Hauschildt[25], C.M. Hawkes[1], R. Hawkings[8], R.J. Hemingway[6], C. Hensel[25], G. Herten[10], R.D. Heuer[25], J.C. Hill[5], K. Hoffman[9], R.J. Homer[1], D. Horváth[29,c], R. Howard[27], P. Hüntemeyer[25], P. Igo-Kemenes[11], K. Ishii[23], H. Jeremie[18], C.R. Jones[5], P. Jovanovic[1], T.R. Junk[6], N. Kanaya[26], J. Kanzaki[23], G. Karapetian[18], D. Karlen[6], V. Kartvelishvili[16], K. Kawagoe[23], T. Kawamoto[23], R.K. Keeler[26], R.G. Kellogg[17], B.W. Kennedy[20], D.H. Kim[19], K. Klein[11], A. Klier[24], S. Kluth[32], T. Kobayashi[23], M. Kobel[3], T.P. Kokott[3], S. Komamiya[23], L. Kormos[26], R.V. Kowalewski[26], T. Krämer[25], T. Kress[4], P. Krieger[6,l], J. von Krogh[11], D. Krop[12], T. Kuhl[25], M. Kupper[24], P. Kyberd[13], G.D. Lafferty[16], H. Landsman[21], D. Lanske[14], J.G. Layter[4], A. Leins[31], D. Lellouch[24], J. Letts[12], L. Levinson[24], J. Lillich[10], C. Littlewood[5], S.L. Lloyd[13], F.K. Loebinger[16], J. Lu[27], J. Ludwig[10], A. Macchiolo[18], A. Macpherson[28,i], W. Mader[3], S. Marcellini[2], T.E. Marchant[16], A.J. Martin[13], J.P. Martin[18], G. Masetti[2], T. Mashimo[23], P. Mättig[24], W.J. McDonald[28], J. McKenna[27], T.J. McMahon[1], R.A. McPherson[26], F. Meijers[8], P. Mendez-Lorenzo[31], W. Menges[25], F.S. Merritt[9], H. Mes[6,a], A. Michelini[2], S. Mihara[23], G. Mikenberg[24], D.J. Miller[15], S. Moed[21], W. Mohr[10], T. Mori[23], A. Mutter[10], K. Nagai[13], I. Nakamura[23], H.A. Neal[33], R. Nisius[8], S.W. O'Neale[1], A. Oh[8], A. Okpara[11], M.J. Oreglia[9], S. Orito[23], C. Pahl[32], G. Pásztor[8,g], J.R. Pater[16], G.N. Patrick[20], J.E. Pilcher[9], J. Pinfold[28], D.E. Plane[8], B. Poli[2], J. Polok[8], O. Pooth[8], A. Quadt[3], K. Rabbertz[8], C. Rembser[8], P. Renkel[24], H. Rick[4], J.M. Roney[26], S. Rosati[3], Y. Rozen[21], K. Runge[10], D.R. Rust[12], K. Sachs[6], T. Saeki[23], O. Sahr[31], E.K.G. Sarkisyan[8,j], A.D. Schaile[31], O. Schaile[31], P. Scharff-Hansen[8], M. Schröder[8], M. Schumacher[3], C. Schwick[8], W.G. Scott[20], R. Seuster[14,f], T.G. Shears[8,h], B.C. Shen[4], C.H. Shepherd-Themistocleous[5], P. Sherwood[15], G. Siroli[2], A. Skuja[17], A.M. Smith[8], R. Sobie[26], S. Söldner-Rembold[10,d], S. Spagnolo[20], F. Spano[9], A. Stahl[3], K. Stephens[16], D. Strom[19], R. Ströhmer[31], S. Tarem[21], M. Tasevsky[8], R.J. Taylor[15], R. Teuscher[9], M.A. Thomson[5], E. Torrence[19], D. Toya[23], P. Tran[4], T. Trefzger[31], A. Tricoli[2], I. Trigger[8], Z. Trócsányi[30,e], E. Tsur[22], M.F. Turner-Watson[1], I. Ueda[23], B. Ujvári[30,e], B. Vachon[26], C.F. Vollmer[31], P. Vannerem[10], M. Verzocchi[17], H. Voss[8], J. Vossebeld[8], D. Waller[6], C.P. Ward[5], D.R. Ward[5], P.M. Watkins[1], A.T. Watson[1], N.K. Watson[1], P.S. Wells[8], T. Wengler[8], N. Wermes[3], D. Wetterling[11] G.W. Wilson[16,k], J.A. Wilson[1], T.R. Wyatt[16], S. Yamashita[23], V. Zacek[18], D. Zer-Zion[4]

[1]School of Physics and Astronomy, University of Birmingham, Birmingham B15 2TT, UK
[2]Dipartimento di Fisica dell' Università di Bologna and INFN, I-40126 Bologna, Italy
[3]Physikalisches Institut, Universität Bonn, D-53115 Bonn, Germany
[4]Department of Physics, University of California, Riverside CA 92521, USA
[5]Cavendish Laboratory, Cambridge CB3 0HE, UK
[6]Ottawa-Carleton Institute for Physics, Department of Physics, Carleton University, Ottawa, Ontario K1S 5B6, Canada
[8]CERN, European Organisation for Nuclear Research, CH-1211 Geneva 23, Switzerland
[9]Enrico Fermi Institute and Department of Physics, University of Chicago, Chicago IL 60637, USA
[10]Fakultät für Physik, Albert Ludwigs Universität, D-79104 Freiburg, Germany
[11]Physikalisches Institut, Universität Heidelberg, D-69120 Heidelberg, Germany
[12]Indiana University, Department of Physics, Swain Hall West 117, Bloomington IN 47405, USA
[13]Queen Mary and Westfield College, University of London, London E1 4NS, UK
[14]Technische Hochschule Aachen, III Physikalisches Institut, Sommerfeldstrasse 26-28, D-52056 Aachen, Germany
[15]University College London, London WC1E 6BT, UK
[16]Department of Physics, Schuster Laboratory, The University, Manchester M13 9PL, UK
[17]Department of Physics, University of Maryland, College Park, MD 20742, USA
[18]Laboratoire de Physique Nucléaire, Université de Montréal, Montréal, Quebec H3C 3J7, Canada
[19]University of Oregon, Department of Physics, Eugene OR 97403, USA
[20]CLRC Rutherford Appleton Laboratory, Chilton, Didcot, Oxfordshire OX11 0QX, UK
[21]Department of Physics, Technion-Israel Institute of Technology, Haifa 32000, Israel
[22]Department of Physics and Astronomy, Tel Aviv University, Tel Aviv 69978, Israel
[23]International Centre for Elementary Particle Physics and Department of Physics, University of Tokyo, Tokyo 113-0033, and Kobe University, Kobe 657-8501, Japan
[24]Particle Physics Department, Weizmann Institute of Science, Rehovot 76100, Israel
[25]Universität Hamburg/DESY, II Institut für Experimental Physik, Notkestrasse 85, D-22607 Hamburg, Germany
[26]University of Victoria, Department of Physics, P O Box 3055, Victoria BC V8W 3P6, Canada
[27]University of British Columbia, Department of Physics, Vancouver BC V6T 1Z1, Canada
[28]University of Alberta, Department of Physics, Edmonton AB T6G 2J1, Canada
[29]Research Institute for Particle and Nuclear Physics, H-1525 Budapest, P O Box 49, Hungary
[30]Institute of Nuclear Research, H-4001 Debrecen, P O Box 51, Hungary
[31]Ludwig-Maximilians-Universität München, Sektion Physik, Am Coulombwall 1, D-85748 Garching, Germany
[32]Max-Planck-Institute für Physik, Föhring Ring 6, 80805 München, Germany
[33]Yale University,Department of Physics,New Haven, CT 06520, USA

[a] and at TRIUMF, Vancouver, Canada V6T 2A3
[b] and Royal Society University Research Fellow
[c] and Institute of Nuclear Research, Debrecen, Hungary
[d] and Heisenberg Fellow
[e] and Department of Experimental Physics, Lajos Kossuth University, Debrecen, Hungary
[f] and MPI München

[g] and Research Institute for Particle and Nuclear Physics, Budapest, Hungary
[h] now at University of Liverpool, Dept of Physics, Liverpool L69 3BX, UK
[i] and CERN, EP Div, 1211 Geneva 23
[j] and Universitaire Instelling Antwerpen, Physics Department, B-2610 Antwerpen, Belgium
[k] now at University of Kansas, Dept of Physics and Astronomy, Lawrence, KS 66045, USA
[l] now at University of Toronto, Dept of Physics, Toronto, Canada

1 Introduction

At LEP2 energies, four-fermion final states with two charged leptons and two neutrinos are dominated by the pair production of W bosons. The probability of both W bosons decaying into leptons is about 10%. These events are characterized by an acoplanar pair of charged leptons in the final state [1]. Systematic uncertainties due to colour reconnection, Bose-Einstein correlations and hadronization modeling, which plague the W mass measurement in other channels, are absent. The full reconstruction of the $\mathrm{W^+W^-} \to \ell\nu\ell'\nu'$ events is not possible due to the presence of at least two unobserved neutrinos in the final state. Therefore the W mass is determined from the energy spectrum of the charged leptons and from an approximate reconstruction of the event referred to as the pseudo-mass method.

This paper presents a measurement of the W mass $\mathrm{M_W}$ in the fully leptonic channel with the Opal detector, using an unbinned maximum likelihood fit. The data sample has an integrated luminosity of 667 $\mathrm{pb^{-1}}$ recorded at center-of-mass energies between 183 GeV and 207 GeV.

A general description of the reconstruction of $\mathrm{W^+W^-} \to \ell\nu\ell'\nu'$ events can be found in [2]. The end-points of the leptonic energy spectrum in $\mathrm{W^+W^-} \to \ell\nu\ell'\nu'$ events depend on the W mass. Neglecting the masses of the charged leptons and the finite width of the W boson, the energy E_ℓ of the charged leptons can be written in terms of $\mathrm{M_W}$ as [1]:

$$\mathrm{E}_\ell = \frac{\sqrt{s}}{4} + \cos\theta^*_\ell \sqrt{\frac{s}{16} - \frac{\mathrm{M_W^2}}{4}} \tag{1}$$

where s is the square of the center-of-mass energy and θ^*_ℓ is the angle between the lepton direction measured in the W rest frame and the direction of the W in the laboratory frame. The latter is not known, so the W mass is determined mainly by the endpoints of the distribution, which correspond to $\cos\theta^*_\ell = \pm 1$. In practice, however, the end-points of the distribution are smeared considerably by the width of the W boson, by initial state radiation and by the detector resolution. These effects weaken the sensitivity of this variable.

In order to include the information from the angle between the two leptons and the correlation between their energies, a second observable based on an approximate kinematic reconstruction of the event — the so-called pseudo-mass — is used in the analysis. The complete reconstruction of the event would require the determination of the four-momenta of both charged leptons and the two neutrinos, 12 quantities in total assuming the masses are known. The four-momenta of the two charged leptons are measured; therefore, the full reconstruction depends on the determination of the momenta of the two neutrinos. Assuming four-momentum conservation and equal masses for the two W bosons, five more constraints can be obtained. An additional arbitrary constraint is imposed to allow the "reconstruction" of the event. By assuming that both neutrinos are in the same plane as the charged leptons, the kinematics can be solved to yield a W *pseudo-mass*, which is quite sensitive to the true W mass. Due to a twofold ambiguity, two solutions are found for this variable:

$$\begin{aligned} M^2_\pm \;=\; & \frac{2}{(\mathbf{p}_{\ell'} + \mathbf{p}_\ell)^2}\Big((P\ \mathbf{p}_{\ell'} - Q\ \mathbf{p}_\ell)(\mathbf{p}_{\ell'} + \mathbf{p}_\ell) \\ & \pm \sqrt{(\mathbf{p}_\ell \times \mathbf{p}_{\ell'})^2 [(\mathbf{p}_{\ell'} + \mathbf{p}_\ell)^2 (E_{\mathrm{beam}} - E_\ell)^2 - (P+Q)^2]} \Big), \end{aligned} \tag{2}$$

[1] The convention c=1 is used throughout this paper.

where

$$P = E_{\rm beam}E_\ell - E_\ell^2 + \frac{1}{2}m_\ell^2, \qquad Q = -E_{\rm beam}E_{\ell'} - \mathbf{p}_{\ell'}\cdot\mathbf{p}_\ell + \frac{1}{2}m_{\ell'}^2,$$

$E_{\rm beam}$ is the beam energy, $E_\ell,\ E_{\ell'}$ are the energies of the two charged leptons, $m_\ell,\ m_{\ell'}$ are their masses and $\mathbf{p}_\ell,\ \mathbf{p}_{\ell'}$ are their three-momenta. In the present analysis the charged leptons are considered to be massless particles because the values of the masses are very small in comparison with their energies. The sensitivity of both solutions was studied with Monte Carlo simulations, which showed that only the larger solution, M_+, is sensitive to $\rm M_W$. The distribution of this solution shows an edge where the value of the pseudo-mass is close to the true W mass.

The pseudo-mass is used here for the first time in determining the W mass in leptonic W-pair decays. It is shown that the correlation between the mass determination from the single lepton energy spectrum and from the pseudo-mass is small, so that the mass measurement can be improved by combining the two methods. For the measurement presented in this paper the total error is dominated by the data statistical error. The largest contributions to the systematic uncertainty in this analysis are due to the uncertainties on the lepton energy which are determined with data and scale with the available statistics. In future experiments with larger statistics it should be possible to reduce both the statistical and systematic uncertainty significantly.

2 Detector Description and Event Selection

A detailed description of the OPAL detector can be found in [3]. The data sample used for this analysis corresponds to an accepted integrated luminosity of 667 $\rm pb^{-1}$, evaluated using small angle Bhabha scattering events observed in the silicon tungsten forward calorimeter [4].

The selection of the $\rm W^+W^- \to \ell\nu\ell'\nu'$ events and the identification of electrons and muons are described in [5,6]. For this analysis events with two charged leptons are required. In view of the experimental problems associated with reconstructing τ-decays, the present analysis is restricted to events which contain at least one W decaying into an electron or a muon for the leptonic energy method (section 3.1.1) and events in which neither of the two W bosons decays into a tau for the pseudo-mass method (section 3.1.2). Table 1 summarizes the signal efficiencies and purities [7]. The dominant background sources are Weν, ZZ and dilepton events. These sources comprise 40%, 30% and 15% of the total background cross-section for the $\rm W^+W^- \to \ell\nu\ell'\nu'$ events [7]. A total of 1101 events for the whole range of center-of-mass energies are observed in the data. Table 2 summarizes the observed numbers of events for each center-of-mass energy together with the corresponding integrated luminosities.

2.1 Monte Carlo Event Generators

At each center-of-mass energy, samples of signal events were generated with five different W masses: 79.33 GeV, 79.83 GeV, 80.33 GeV, 80.83 GeV and 81.33 GeV. In the range of 183–189 GeV, samples corresponding to the central value of 80.33 GeV were generated according to the CC03 [2] diagrams with KORALW [9], $\rm e^+e^- \to ZZ$ and Zee background events were generated with PYTHIA [10] and Weν with KORALW [9] . For the other W masses and for center-of-mass energies in the range of 192–207 GeV KORALW was used both for the signal and for these

[2]The leading order $\rm W^+W^-$ production diagrams, i.e. the t-channel $\nu_{\rm e}$ exchange and the s-channel $\rm Z^0/\gamma$ exchange, are referred to as CC03, following the notation of [8].

four-fermion backgrounds. Other backgrounds were simulated by RADCOR [11] for multi-photon final states, KORALZ [12] and BHWIDE [13] for dilepton final states and two-photon events were simulated with VERMASEREN [14] and HERWIG [15]. Finally YFSWW3 [16] samples were used to perform systematic studies related to photon radiation in W^+W^- events.

2.2 Classification of Events

The momentum resolutions obtainable with OPAL for electrons and muons differ significantly at high energies. For electrons, the preferred measurement uses the electromagnetic calorimeter energy information which has a resolution of approximately 3% at 45 GeV, whereas for muons at the same energy, the charged particle momentum determined in the central tracker has a resolution of approximately 8% [17]. Therefore, to maximize the sensitivity of the measurement, electrons and muons are treated separately by defining different classes of events for the leptonic energy and the pseudo-mass analyses, depending upon the identified lepton flavours. Identified taus are rejected since their energy cannot be determined.

In the case of the leptonic energy the information of both charged leptons is used independently. For this variable two different classes are defined: the first class contains leptons identified as electrons and the second class contains leptons identified as muons. To increase the number of leptons used in the analysis, the higher energy identified electrons or muons in events selected as either $e\nu_e\tau\nu_\tau$ or $\mu\nu_\mu\tau\nu_\tau$ are also used.

For the pseudo-mass three classes of events are defined as follows:

1. Events consisting of two leptons identified as e.
2. Events consisting of two leptons identified as μ.
3. Events consisting of two leptons identified as an e and a μ.

Table 3 shows the classification of events for the leptonic energy and the pseudo-mass. The number of leptons selected for the leptonic energy method, and the number of events selected for the pseudo-mass method are summarized in Table 2.

3 Extraction of the W Mass

3.1 Unbinned Maximum Likelihood Method

The extraction of the W mass was performed by a simultaneous maximum likelihood fit to the leptonic energy and the pseudo-mass distributions using the data from center-of-mass energies from 183 GeV to 207 GeV. The fit is performed with the following product of likelihood functions:

$$\mathcal{L}_T = \prod_{k=1}^{8} \left(\prod_{i=1}^{2} \mathcal{L}_{LE}^{k} \times \prod_{i=1}^{3} \mathcal{L}_{PM}^{k} \right) \tag{3}$$

where k denotes the eight center-of-mass energies included in the fit and i runs over the two classes defined for the leptonic energy (LE) and the three classes defined for the pseudo-mass (PM).

The leptonic energy and the pseudo-mass distributions obtained from Monte Carlo simulations (including all background sources) are parameterized by appropriate analytic functions,

$$f = f(P_1, \cdots, P_N; x), \tag{4}$$

which depend on N parameters, P_i, and on the variable x, which stands for either the leptonic energy or the pseudo-mass. For each parameter a linear dependence on $\mathrm{M_W}$ is assumed:

$$P_i = b_i^0 + b_i^1 \times \mathrm{M_W} \tag{5}$$

The coefficients b_i^0 and b_i^1 are obtained by fitting the analytic functions to the leptonic energy and the pseudo-mass spectra generated at different W masses. The coefficient b_i^1 is included only if it is not compatible with zero within one standard deviation (i.e. its numerical value is larger than the corresponding error); otherwise only a constant term is used. This parameterization is performed independently for each class defined for the sensitive variables. Details of the method are discussed in the following sections.

3.1.1 Parameterization of the Leptonic Energy

The leptonic energy spectrum is fitted with a function f_T, which is the product of two Fermi functions and a linear function:

$$f_T = f_1 \times f_2 \times f_3 \tag{6}$$

with

$$f_1 = \frac{1}{e^{-\frac{x-P_1}{P_2}}+1}, \quad f_2 = P_5(1+P_6\times x), \quad f_3 = \frac{1}{e^{\frac{x-P_3}{P_4}}+1}. \tag{7}$$

P_1 and P_3 correspond to the points of inflection of the two Fermi functions, P_2 and P_4 to their widths, P_5 is the constant term of the linear function and the slope is proportional to P_6.

The fit function depends therefore on six parameters. The overall normalization of the spectra can be used to eliminate P_5. For each set of values of the P_1, P_2, P_3, P_4 and P_6 parameters, P_5 is calculated so that the total function is normalized in the region taken to perform the fit. The lower limit is 10 GeV for all center-of-mass energies and the upper limit changes depending on the center-of-mass energy from 80 GeV for 183 GeV to 100 GeV for 207 GeV. The regions at the end-points of the leptonic energy spectrum are sensitive to $\mathrm{M_W}$. In terms of the parameterization these edges correspond to P_1 and P_3. These are the only parameters which are expected to change with the W mass while the other parameters, P_2, P_4 and P_6, are more sensitive to the W width and detector resolution effects. This has been confirmed by studying the linear dependence of each parameter on $\mathrm{M_W}$. Figure 1 shows an example of a fit to the leptonic energy distribution. The spectrum is generated from a Monte Carlo sample with a W mass of 80.33 GeV at a center-of-mass energy of 189 GeV.

A simultaneous fit of the parameters $P_1(\mathrm{M_W})$, P_2 and $P_3(\mathrm{M_W})$, P_4 and P_6 with the Monte Carlo samples for different values of $\mathrm{M_W}$ is performed. Parameters P_2, P_4 and P_6 are assumed to be independent of $\mathrm{M_W}$ and a common value is determined for each of these. P_1 and P_3 describe the $\mathrm{M_W}$ dependence and a separate value is determined for each generated $\mathrm{M_W}$. Figure 2 shows the fitted parameters P_1 and P_3 and the linear dependence on $\mathrm{M_W}$ for the case of electrons. These fits are performed independently for each class of events and each center-of-mass energy.

3.1.2 Parameterization of the Pseudo-mass

The analytic function chosen to fit the pseudo-mass spectra is the sum of a Fermi function and a constant function, with four free parameters:

$$f = P_1 \left(\frac{1}{e^{-\frac{x-P_2}{P_3}} + 1} + P_4 \right). \quad (8)$$

P_1, P_2 and P_3 are proportional to the amplitude of the curve, to the point of inflection of the slope and to the width respectively and P_4 is a constant term. As with the lepton energy, one parameter can be eliminated due to the constraint of the overall normalization. This procedure is used to eliminate the parameter P_1. For each set of values of the P_2, P_3, P_4 parameters, P_1 is determined to normalize the function within the fit range of 70 GeV to 90 GeV, which is the same for all center-of-mass energies. In terms of the above parameterization, the edge of the pseudo-mass distribution corresponds to P_2. This is the only parameter which is expected to show a clear dependence on M_W. Figure 3 shows an example of the function fitted to a simulated pseudo-mass distribution. Similar fits are performed for each class of events at all center-of-mass energies considered in the analysis. The edge around the generated W mass can be observed in the figure. The individual linear dependence of each parameter on M_W was studied in the same way as for the leptonic energy. In this case, a simultaneous fit of the parameters $P_2(M_W)$, P_3 and P_4 with the Monte Carlo samples for the different values of M_W was performed. P_3 and P_4 are found to be independent of M_W; therefore a common value was determined for each. P_2 describes the M_W dependence and an independent value was determined for each generated M_W. Figure 4 shows the fitted values of the P_2 parameter and its linear dependence on M_W in the case of electron-electron events.

3.2 Monte Carlo Studies

The correlation between the fitted masses for the leptonic energy and for the pseudo-mass has been determined to be $(11 \pm 1)\%$, considering all center-of-mass energies together. This was evaluated by fitting the W mass separately for the leptonic energy and the pseudo-mass with an ensemble of 90 independent data-sized Monte Carlo subsamples generated with a W mass of 80.33 GeV.

The simultaneous fit method has been tested with 2000 data-size experiments derived by resampling from Monte Carlo simulations. The events of these subsamples were picked at random from the full Monte Carlo sample, whose signal part (generated at $M_W = 80.33$ GeV) corresponded to 90 times the data statistics. Multiple draws of the same events were allowed. Figure 5(a) shows the results of the resampling tests fitted with a Gaussian function. The pull distribution is shown in figure 5(b). To compensate for the underestimation of the statistical error by the common fit due to the correlation between the leptonic energy and the pseudo-mass, the errors of the fit used in the pull distribution have been increased by a factor 1.11.

3.2.1 Bias Test

The method presented to extract the W mass is not expected to show any bias. Possible biases due to detector effects are eliminated since these are simulated with Monte Carlo methods. Biases related to the selection of the analytic functions which fit the leptonic energy and the pseudo-mass are negligible as long as the functions fit the variables properly. By using Monte Carlo samples generated with $M_W = 79.33$, 79.83, 80.33, 80.83 and 81.33 GeV, the bias and the linearity can be determined. First, the individual relations between the generated and the fitted masses are studied independently for the leptonic energy and for the pseudo-mass. The distributions show slopes and biases compatible with one and zero respectively, 0.958 ± 0.087

and -0.061 ± 0.054 GeV for the leptonic energy and 0.952 ± 0.086 and -0.031 ± 0.044 GeV for the pseudo-mass. Second, the relation between the generated and the fitted mass is studied for the simultaneous fit to both the leptonic energy and the pseudo-mass. This relation is shown in Figure 6 and found to be linear in a region of $\pm$ 1 GeV from the central value of 80.33 GeV, with a slope of 0.983 ± 0.063 and a bias value of -0.055 ± 0.031 GeV. No corrections are included due to the slope or bias values since there is no evidence of a bias.

4 Fit Results and Discussion

The simultaneous fit to the data distribution of the leptonic energy and the pseudo-mass, combining center-of-mass energies from 183 GeV to 207 GeV, gives the following result:

$$\mathrm{M_W} = 80.41 \pm 0.41 \text{ GeV},$$

where the quoted error is statistical only and has been scaled by a factor 1.11 to take into account the correlation between the two variables. The W mass values obtained separately are $\mathrm{M_W} = 80.58 \pm 0.52$ GeV for the leptonic energy and $\mathrm{M_W} = 80.20 \pm 0.61$ GeV for the pseudo-mass. Figure 7 shows the comparison between the fit function and the data for the two classes defined for the leptonic energy at a center-of-mass energy of 207 GeV. The poorer resolution of the muon energy compared to the electron energy is visible in the fit functions. The regions around the end-points have sharper edges for electrons than for muons. Figure 8 shows analogous results for the three classes of events defined for the pseudo-mass at all center-of-mass energies. The greater sensitivity of electron-electron events relative to muon-muon or electron-muon events can be observed by comparing the fit functions around 80 GeV, i.e. in the region sensitive to $\mathrm{M_W}$.

5 Systematic Checks and Uncertainties

The study of the systematic uncertainties on the W mass is described in this section and summarized in Table 4. The sources of systematic errors have been studied simultaneously for all center-of-mass energies. The total systematic error is calculated as a quadratic sum of the contributions listed below.

5.1 Beam Energy

The average LEP beam energy is currently known with a precision of about $\pm$ 20 MeV, varying slightly for different center-of-mass energies between 183 GeV and 207 GeV [18]. This leads to a systematic uncertainty of 11 MeV. The RMS spread in the LEP center-of-mass energy is around 240 MeV, varying slightly with the center-of-mass energy. The systematic error due to the uncertainty of the beam energy spread is 3 MeV. In addition the data at average center-of-mass energies of 205 GeV and 207 GeV were taken at a number of discrete energy points in the range of 204.6–206.0 GeV and 206.2–208.0 GeV, respectively. This leads to a bias of 12 MeV for which the fit result has been corrected. The average difference between the electron and the positron beam energies has negligible impact on the measurement of $\mathrm{M_W}$.

5.2 QED Corrections

The systematic error associated with uncertainties in the modeling of the QED corrections is estimated by reweighting events generated with YFSWW3, which has a more complete treatment of $\mathcal{O}(\alpha)$ QED corrections, according to KORALW probabilities. The corresponding difference of 7 MeV is taken as systematic error.

5.3 Detector and Resolution Effects

The effects of the detector calibrations and the deficiencies in the Monte Carlo simulation of the detector response are investigated by varying the observed leptonic energy scales in the electromagnetic calorimeter (for the electrons) and in the central tracker (for the muons) over reasonable ranges [19]. The ranges used for the systematic variations depend on the polar angle and are determined from detailed comparisons of data and Monte Carlo utilizing both data recorded at 189–207 GeV and data collected at $\sqrt{s} \approx M_Z$ during 1998–2001. Due to differences observed in the resolution between the data and the Monte Carlo simulation during these years, correction factors for electron and muon energy are included in the reference samples. The difference between the measured and the generated energy is scaled by a factor 1.07 for the electromagnetic calorimeter and 1.06 for the central tracker.

From the systematic studies of the lepton energy scale, the electromagnetic calorimeter energy scales and the central tracker scale are both known to 0.3%. These scale uncertainties dominate the detector related systematics in the $W^+W^- \to \ell\nu\ell'\nu'$ channel. For muons the scale uncertainty is 32 MeV. In the case of electrons, the scale errors are expected to be uncorrelated between the barrel and endcap regions and therefore the analysis for electrons was performed separately in both regions and combined in quadrature, resulting in an uncertainty of 85 MeV. The systematic uncertainty due to the non-linearity in the electromagnetic calorimeter and the central tracker is taken into account by varying the energy using a factor which changes linearly from -0.1% to 0.1% in the range 20–70 GeV. The corresponding systematic error is 43 MeV for electrons and 33 MeV for muons.

The systematic error due to the uncertainties on the resolution is studied with Monte Carlo samples by comparing the fitted W mass with the nominal resolution to that with resolutions changed by 1.10 for electrons (with the information of the electromagnetic calorimeter) and 1.07 for muons (with the information of the central tracker). The corresponding errors are 43 MeV and 12 MeV respectively.

5.4 Background Treatment

The background normalization is varied by $\pm$ 5%, which corresponds to the error in the cross section measurement for the leptonic channel [7]. The resulting change in the fitted M_W is 11 MeV.

5.5 Parameterization of the Sensitive Variables

A total of 152 parameters are obtained for the leptonic energy and the pseudo-mass considering center-of-mass energies from 183 GeV to 207 GeV for all the defined classes. From these, 56 parameters depend on the mass of the W boson. To check the systematic error associated with the parameterization of the leptonic energy and the pseudo-mass distributions each parameter is varied independently by $\pm 1\sigma$. This is repeated for all center-of-mass energies and all

classes defined for the leptonic energy and for the pseudo-mass. Adding the resulting changes in quadrature yields a total systematic uncertainty due to the parameterization of 51 MeV.

Since the parameterization of the pseudo-mass does not describe a possible fall of the distribution above 85 GeV we tried an alternative parameterization by multiplying the standard parameterization by a linear function. This changes the fit result by 4 MeV.

5.6 Four-Fermion Effects

Using events generated according to the CC03 diagrams instead of the full set of four-fermion diagrams results in a mass bias of 24 MeV. This has been determined by reweighting events produced with KoralW to the prediction of the CC03 matrix element. The fit result has been corrected for the mass bias due to the use of the CC03 Monte Carlo at center-of-mass of 183 GeV and 189 GeV. The remaining uncertainty due to the modeling of the four fermion final state is expected to be significantly smaller and has been neglected in the estimation of the total systematic uncertainty.

6 Outlook for Future Experiments

This analysis has demonstrated for the first time that the correlation between the two leptons can be used as additional information to the single lepton energy spectra in the determination of the W mass from leptonic W-pair decays. Due to the small correlation between the mass determination from the pseudo-mass and from the lepton energy the uncertainty is reduced significantly by combining the two measurements. The systematic uncertainty could be significantly reduced in future high-statistics experiments. The uncertainties on the energy scale, resolution and linearity are determined with data and scale with the available statistics. The error due to the parameterization depends on the number of available Monte Carlo events and can be kept small by producing sufficiently large samples.

The different sensitivities of the edges of lepton energy distributions and the pseudo-mass to the beam energy result in a reduced systematic error from the uncertainty in the beam energy in this analysis compared to the $W^+W^- \to q\bar{q}\ell\nu$ and $W^+W^- \to q\bar{q}q\bar{q}$ channels [19]. This will be important at future colliders, where the beam energy measurements will be one of the limiting systematic uncertainties.

For the $W^+W^- \to q\bar{q}\ell\nu$ and $W^+W^- \to q\bar{q}q\bar{q}$ channels the hadronisation of the quarks gives rise to an important systematic uncertainty which can only be estimated by the comparison of different hadronisation models. The determination of the W mass in purely leptonic W decays is free from this uncertainty. As discussed, the total error in this channel should be competitive with the $W^+W^- \to q\bar{q}\ell\nu$ and $W^+W^- \to q\bar{q}q\bar{q}$ channels with sufficiently high statistics.

7 Summary

The energy of the leptons produced in the reaction $e^+e^- \to W^+W^- \to \ell\nu\ell'\nu'$ and the pseudo-mass, a variable which is based on an approximate kinematic reconstruction of the event, are used to measure the mass of the W boson. Both variables are combined in a simultaneous unbinned maximum likelihood fit, using data collected at center-of-mass energies between 183 GeV and 207 GeV. The following result is obtained:

$$M_W = 80.41 \pm 0.41 \pm 0.13 \text{ GeV},$$

where the first uncertainty quoted is statistical and the second is systematic. The result obtained is consistent with previous measurements of M_W [19, 20].

8 Acknowledgements

We particularly wish to thank the SL Division for the efficient operation of the LEP accelerator at all energies and for their close cooperation with our experimental group. We thank our colleagues from CEA, DAPNIA/SPP, CE-Saclay for their efforts over the years on the time-of-flight and trigger systems which we continue to use. In addition to the support staff at our own institutions we are pleased to acknowledge the
Department of Energy, USA,
National Science Foundation, USA,
Particle Physics and Astronomy Research Council, UK,
Natural Sciences and Engineering Research Council, Canada,
Israel Science Foundation, administered by the Israel Academy of Science and Humanities,
Minerva Gesellschaft,
Benoziyo Center for High Energy Physics,
Japanese Ministry of Education, Science and Culture (the Monbusho) and a grant under the Monbusho International Science Research Program,
Japanese Society for the Promotion of Science (JSPS),
German Israeli Bi-national Science Foundation (GIF),
Bundesministerium für Bildung und Forschung, Germany,
National Research Council of Canada,
Research Corporation, USA,
Hungarian Foundation for Scientific Research, OTKA T-029328, T023793 and OTKA F-023259,
Fund for Scientific Research, Flanders, F.W.O.-Vlaanderen, Belgium.

References

[1] Physics at LEP2, CERN 96–01, ed. G. Altarelli *et al.*, Vol 1 (1996), published at CERN.

[2] K. Hagiwara, R.D. Peccei, D. Zeppenfeld and K. Hikasa, Nucl. Phys., **B282** (1987) 253.

[3] OPAL Collab., K. Ahmet *et al.*, Nucl. Instr. Meth. **A305** (1991) 275;
B. E. Anderson *et al.*, IEEE Transactions on Nuclear Science, **41** (1994) 845;
S. Anderson *et al.*, Nucl. Instr. Meth., **A403** (1998) 326.

[4] OPAL Collab., G. Abbiendi *et al.*, Eur. Phys. J., **C13** (2000) 553.

[5] The selection is an improved version of Selection II described in
OPAL Collab., K. Ackerstaff *et al.*, Eur. Phys. J., **C14** (2000) 51.

[6] OPAL Collab., K. Ackerstaff *et al.*, Eur. Phys. J., **C4** (1998) 47.

[7] OPAL Collab., G. Abbiendi *et al.*, Phys. Lett., **B493** (2000) 249.

[8] Physics at LEP2, CERN 96–01, ed. G. Altarelli *et al.*, Vol 2 (1996), published at CERN.

[9] M. Skrzypek *et al.*, Comp. Phys. Comm., **94** (1996) 216;
M. Skrzypek *et al.*, Phys. Lett., **B372** (1996) 289;
S. Jadach *et al.*, Comp. Phys. Comm., **119** (1999) 272.

[10] T. Sjöstrand, Comp. Phys. Comm., **82** (1994) 74.

[11] F.A. Berends and R. Kleiss, Nucl. Phys., **B186** (1981) 22.

[12] S. Jadach, B.F.L. Ward and Z. Wąs, Comp. Phys. Comm., **79** (1994) 503.

[13] S. Jadach, W. Placzek and B.F.L. Ward, Phys. Lett., **B390** (1997) 298.

[14] J.A.M Vermaseren, Phys. Lett., **B229** (1983) 347.

[15] G. Marchesini, *et al.*, Comp. Phys. Comm., **67** (1992) 465.
G. Marchesini, *et al.*, preprint hep–ph/9607393.

[16] S. Jadach *et al.*, Comp. Phys. Comm., **140** (2001) 432.

[17] OPAL Collab., K. Ahmet *et al.*, Nucl. Instr. Meth., **A305** (1991) 275.

[18] G. Wilkinson, LEP Energy Working Group, *Private communication.*
A. Blondel, *et al.*, LEP Energy Working Group, Eur. Phys. J., **C11** (1999) 573.

[19] OPAL Collab., G. Abbiendi *et al.*, Phys. Lett., **B507** (2001) 29.

[20] The LEP Collaborations: ALEPH, DELPHI, L3, OPAL, the LEP Electroweak Working Group, and the SLD Heavy Flavour and Electroweak Groups, CERN-EP-2001-098 (2001).
D.G. Charlton, 'Experimental tests of the Standard Model', proceedings of International Europhysics Conference on High Energy Physics, 2001, Budapest (Hungary), PRHEP-hep 2001/285.

Event	Efficiency (%)	Purity (%)
$e\nu_e e\bar{\nu}_e$	75.5	91.2
$\mu\nu_\mu\mu\bar{\nu}_\mu$	80.4	90.9
$e\nu_e\mu\bar{\nu}_\mu$	77.8	95.9
$e\nu_e\tau\bar{\nu}_\tau$	60.3	71.9
$\mu\nu_\mu\tau\bar{\nu}_\tau$	60.6	75.5

Table 1: Signal efficiencies and purities for the leptonic events used in the analysis.

Center-of-mass energy (GeV)	Integrated Luminosity (pb^{-1})	Number of $W^+W^- \to \ell\nu\ell'\nu'$ events	Number of leptons —leptonic energy—	Number of events —pseudo-mass—
183	57	71	77	26
189	183	278	309	80
192	29	52	51	12
196	77	144	169	32
200	74	134	144	25
202	37	82	87	16
205	82	129	141	14
207	128	211	248	29
All	667	1101	1226	234

Table 2: Integrated luminosities for the data from 183 to 207 GeV. The total number of events selected as $W^+W^- \to \ell\nu\ell'\nu'$, the number of leptons used for the leptonic energy and the number of events used for the pseudo-mass are shown.

	e	μ	τ
e	LE/PM	LE/PM	LE
μ	LE/PM	LE/PM	LE
τ	LE	LE	–

Table 3: Classification of events used for the leptonic energy (LE) and the pseudo-mass (PM) analysis.

Systematic errors	Error (GeV)
Beam energy	0.011
Spread in the beam energy	0.003
QED Corrections	0.007
Electromagnetic calorimeter scale	0.085
Electromagnetic calorimeter resolution	0.043
Electromagnetic calorimeter linearity	0.043
Central tracker scale	0.032
Central tracker resolution	0.012
Central tracker linearity	0.033
Background	0.011
Parameterization	0.051
Total	0.127

Table 4: Summary of systematic uncertainties on the M_W measurement.

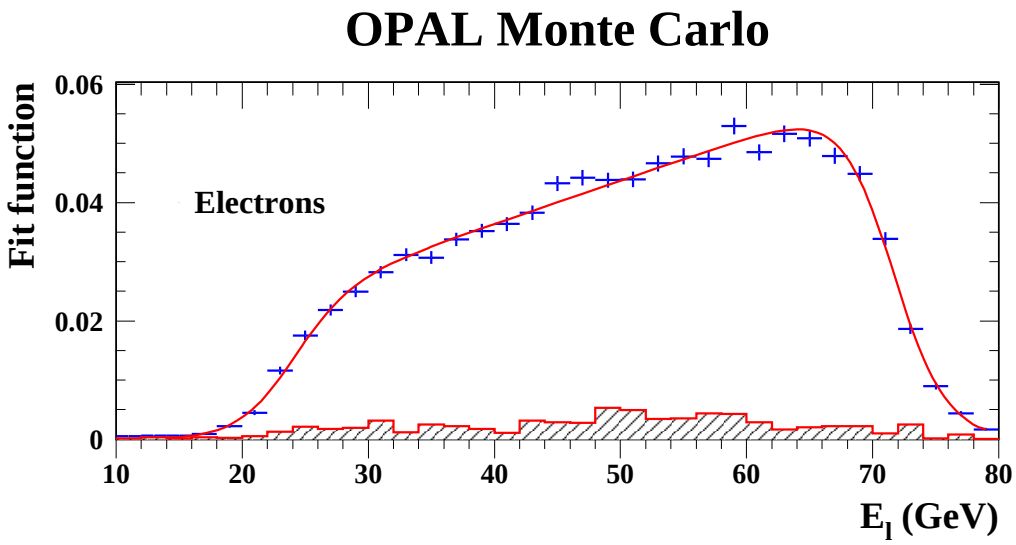

Figure 1: Fit to the leptonic energy distribution generated with $M_W = 80.33$ GeV for $\sqrt{s} = 189$ GeV. The crosses indicate Monte Carlo events and the shaded area shows the background Monte Carlo. Only leptons tagged as electrons were used for this distribution. The fitted function has five free parameters and is a product of two Fermi functions and a linear function.

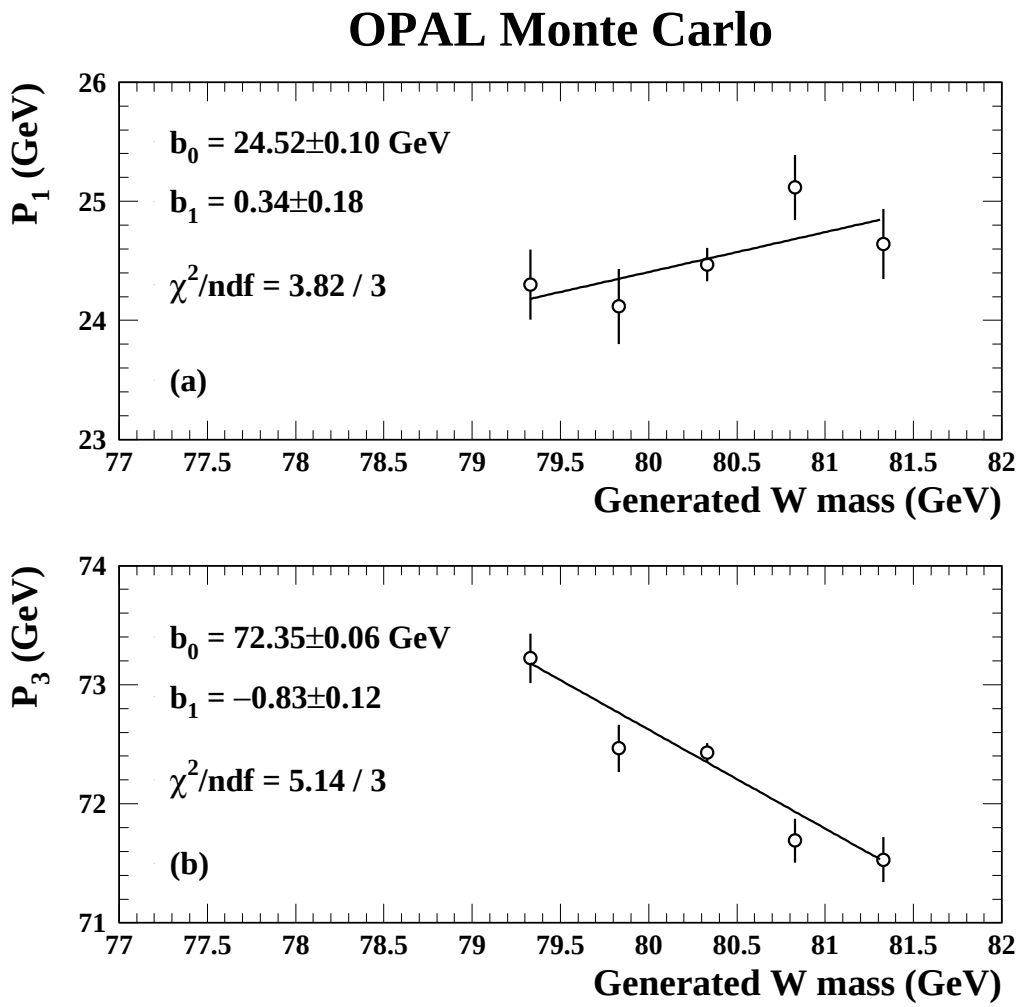

Figure 2: Linear fit ($P_i = b_0 + b_1 \times (\mathrm{M_W} - 80.33)$) of the coefficients (a) P_1 and (b) P_3 (points of inflection of the Fermi functions) at a center-of-mass energy of 189 GeV. The events chosen to perform this fit belong to the first class defined for the leptonic energy, which contains electrons only. Similar studies are performed for the second class and at all center-of-mass energies.

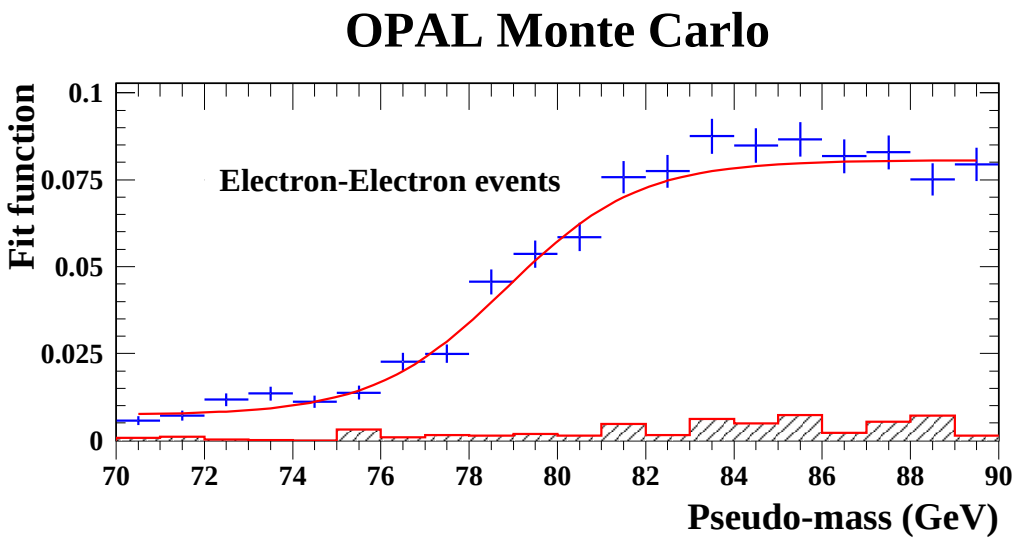

Figure 3: Fit to the pseudo-mass distribution generated with $M_W = 80.33$ GeV for $\sqrt{s} = 189$ GeV. The crosses indicate simulated Monte Carlo events and the shaded area shows the background Monte Carlo. Only events tagged as electron-electron were used. The fitted function has three free parameters and consists of a Fermi function plus a constant.

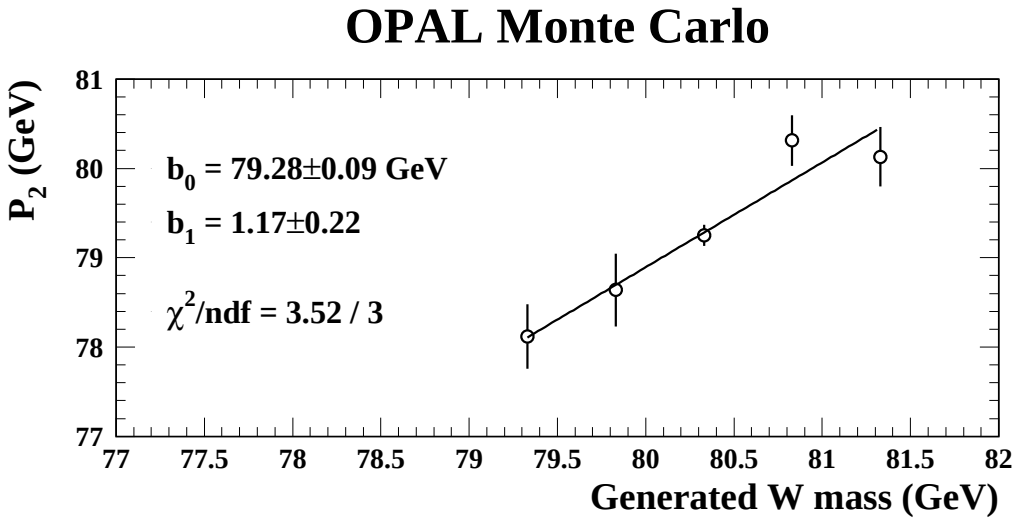

Figure 4: Linear fit ($P_2 = b_0 + b_1 \times (M_W - 80.33)$) of the coefficient P_2 (point of inflection of the Fermi function) to M_W at a center-of-mass energy of 189 GeV. The events chosen to perform this fit belong to the first class defined for the pseudo-mass, which contains electrons only. Similar studies are performed for the second and third classes and at all center-of-mass energies.

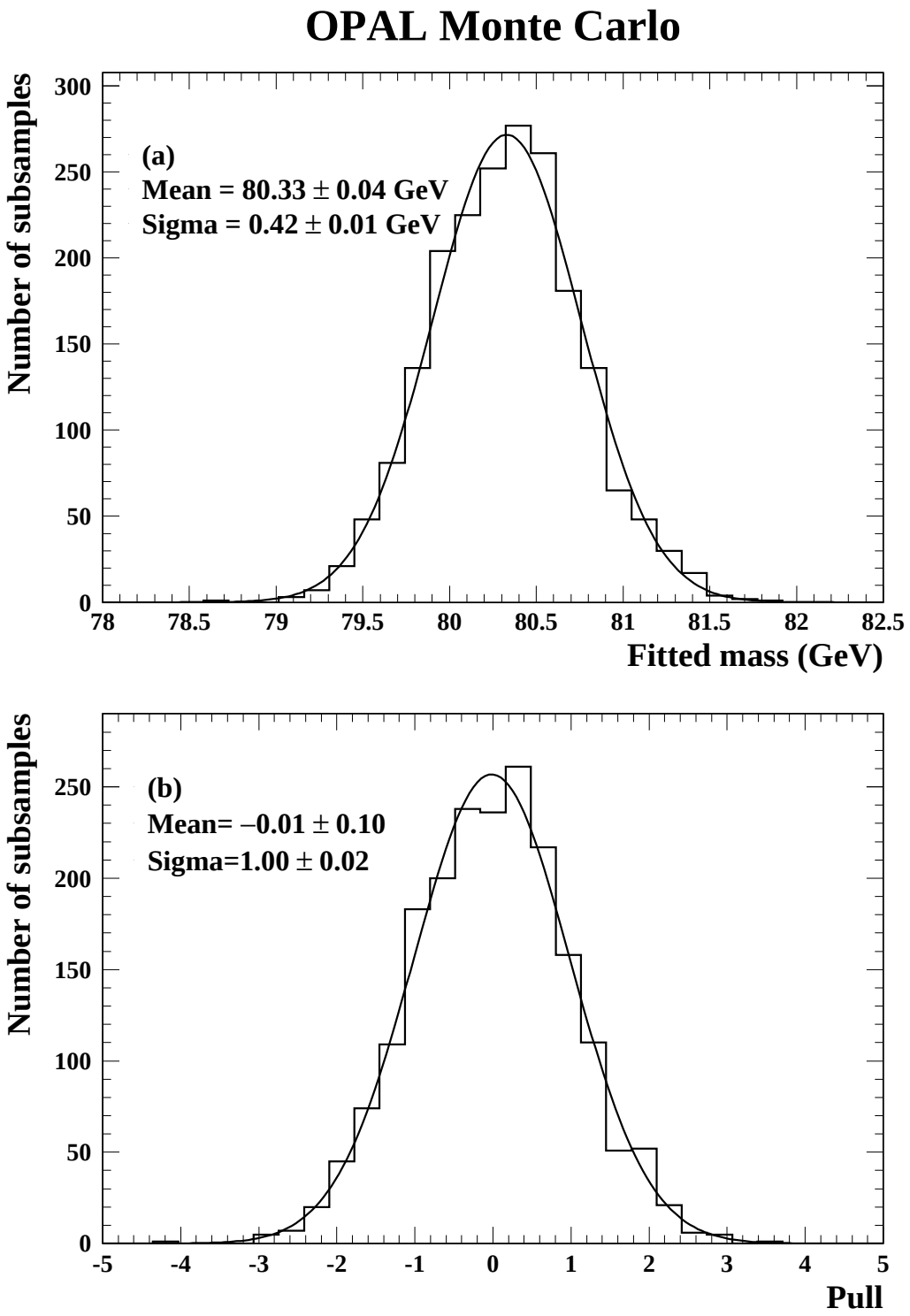

Figure 5: (a) Fitted mass distribution from Monte Carlo for the simultaneous fit of the leptonic energy and the pseudo-mass at all center-of-mass energies. The test samples are generated at $M_W = 80.33$ GeV. (b) The corresponding pull distribution. The errors have been rescaled by a factor 1.11 to take into account the correlation between the leptonic energy and the pseudo-mass.

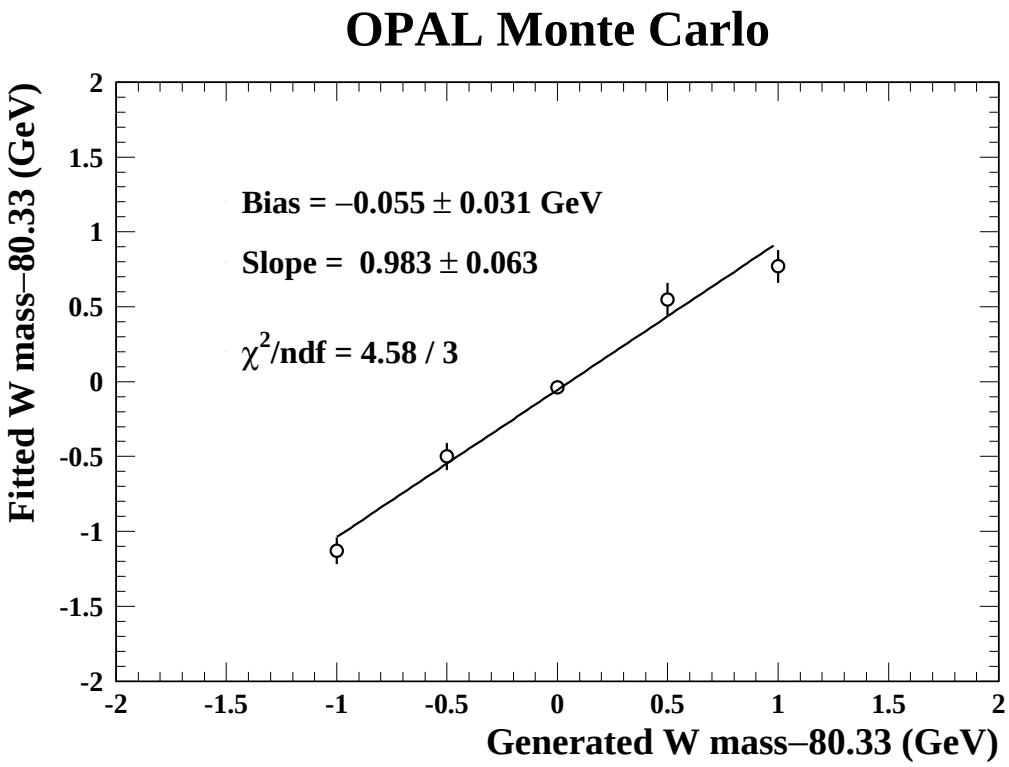

Figure 6: Fitted versus generated W mass, showing the linearity of the unbinned method. The central value of 80.33 GeV is subtracted from all the masses.

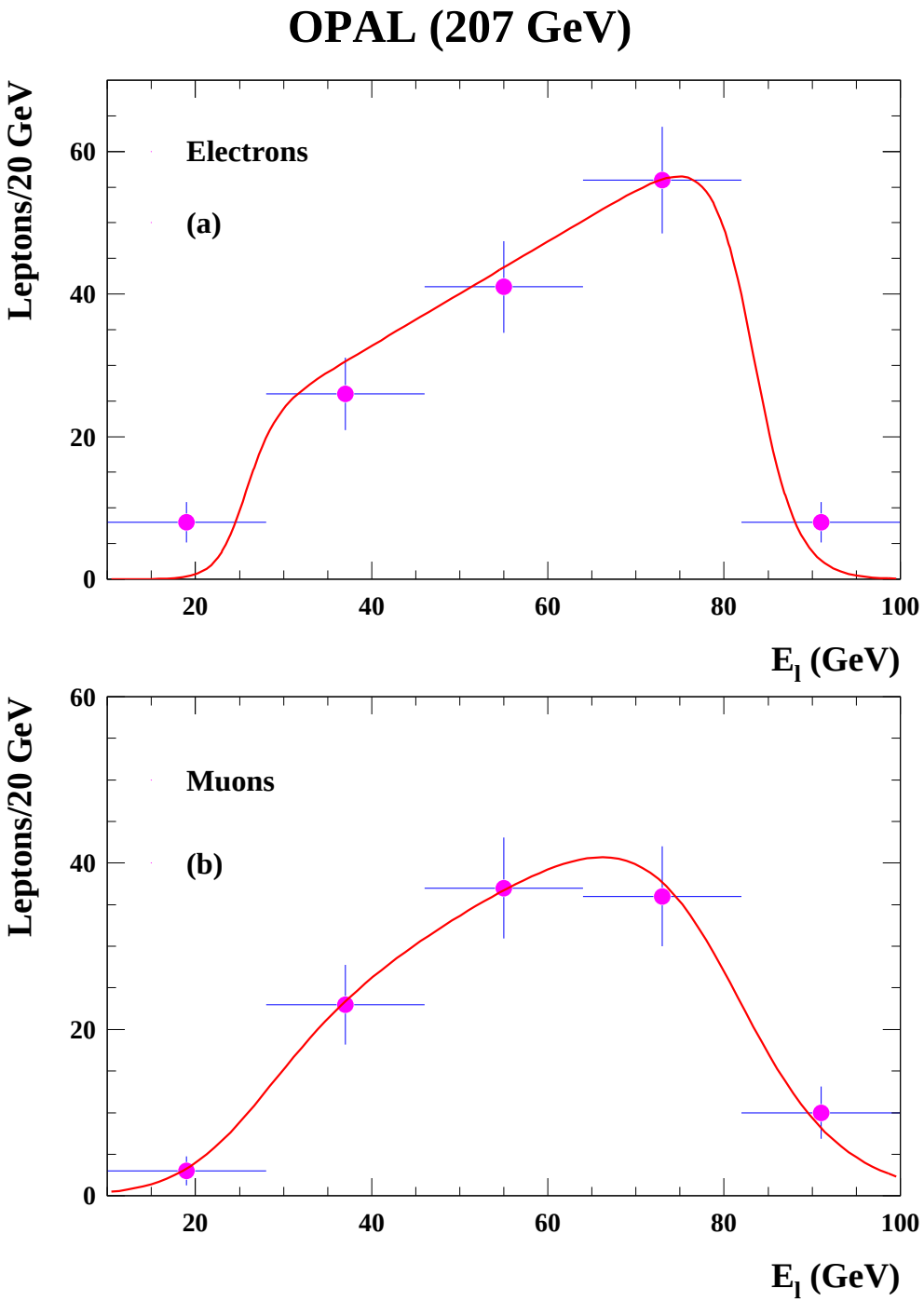

Figure 7: Comparison between the data and the fit functions for the leptonic energy at a center-of-mass energy of 207 GeV. (a) electrons. (b) muons.

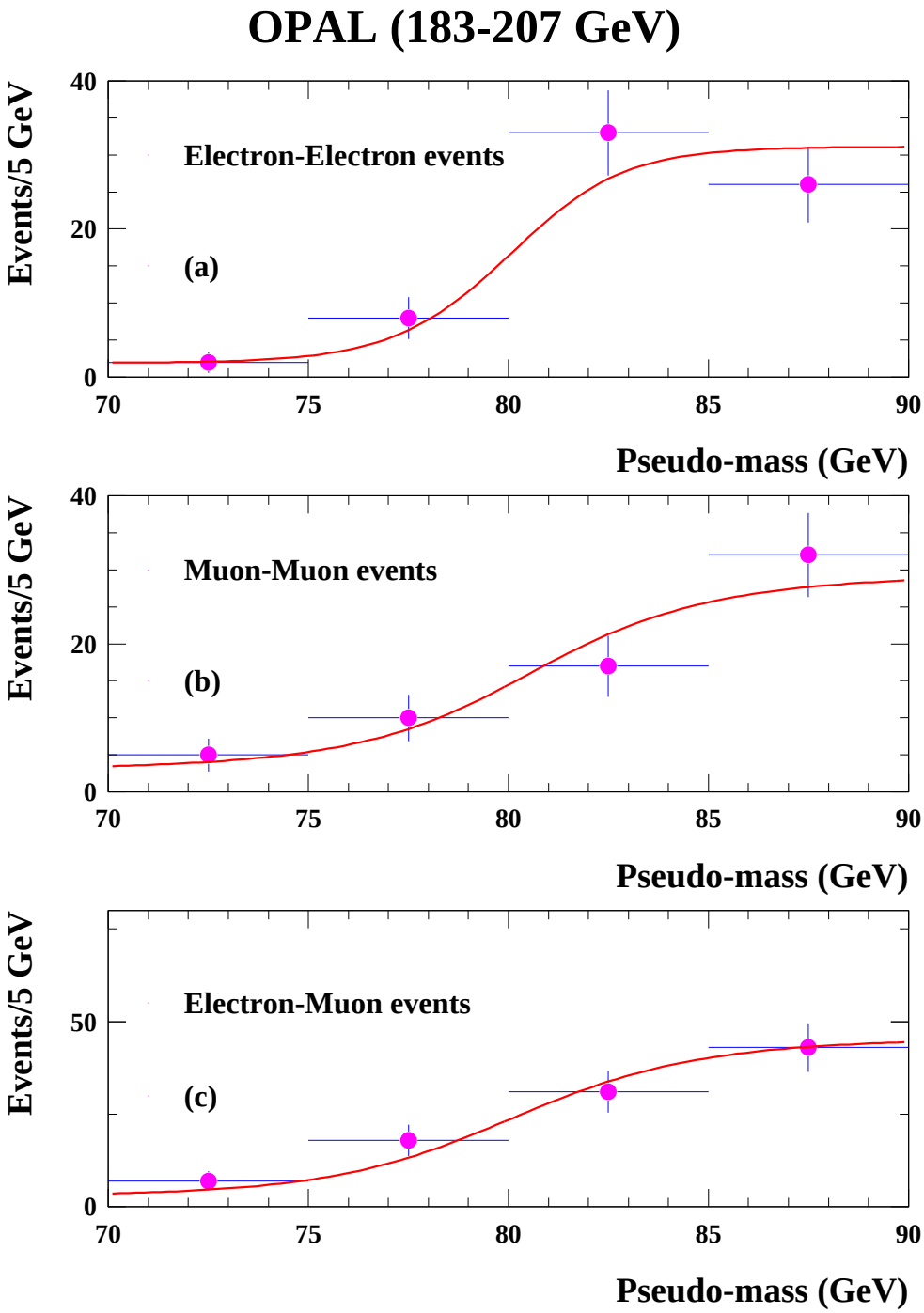

Figure 8: Comparison between the data and the fit function for the pseudo-mass at all center-of-mass energies. (a) electron-electron events. (b) muon-muon events. (c) electron-muon events.